LOCKHEED MARTIN ENERGY RESEARCH LIBRARIES
3 4456 0443705 4

CENTRAL RESEARCH LIBRARY
DOCUMENT COLLECTION

39

ORNL-3542
UC-80 – Reactor Technology
TID-4500 (26th ed.)

EFFECTS OF TEMPERATURE ON FISSION-PRODUCT DEPOSITION

M. N. Ozisik

OAK RIDGE NATIONAL LABORATORY
operated by
UNION CARBIDE CORPORATION
for the
U.S. ATOMIC ENERGY COMMISSION

CENTRAL RESEARCH LIBRARY
DOCUMENT COLLECTION
LIBRARY LOAN COPY
DO NOT TRANSFER TO ANOTHER PERSON
If you wish someone else to see this
document, send in name with document
and the library will arrange a loan.

Printed in USA. Price: $0.75 Available from the
Office of Technical Services
U. S. Department of Commerce
Washington 25, D. C.

LEGAL NOTICE

This report was prepared as an account of Government sponsored work. Neither the United States, nor the Commission, nor any person acting on behalf of the Commission:

A. Makes any warranty or representation, expressed or implied, with respect to the accuracy, completeness, or usefulness of the information contained in this report, or that the use of any information, apparatus, method, or process disclosed in this report may not infringe privately owned rights; or

B. Assumes any liabilities with respect to the use of, or for damages resulting from the use of any information, apparatus, method, or process disclosed in this report.

As used in the above, "person acting on behalf of the Commission" includes any employee or contractor of the Commission, or employee of such contractor, to the extent that such employee or contractor of the Commission, or employee of such contractor prepares, disseminates, or provides access to, any information pursuant to his employment or contract with the Commission, or his employment with such contractor.

ORNL-3542

Contract No. W-7405-eng-26

Reactor Division

EFFECTS OF TEMPERATURE ON FISSION-PRODUCT DEPOSITION

M. N. Ozisik

MARCH 1964

OAK RIDGE NATIONAL LABORATORY
Oak Ridge, Tennessee
operated by
UNION CARBIDE CORPORATION
for the
U.S. ATOMIC ENERGY COMMISSION

LOCKHEED MARTIN ENERGY RESEARCH LIBRARIES
3 4456 0443705 4

CONTENTS

	Page
Abstract	1
Introduction	1
Nomenclature	2
Basic Considerations	3
Derivation of Equations	4
Coolant Velocity, U	8
Mass Transfer Coefficient, C	8
Probability Factor, P	10
Diffusion Ratio, K	13
Computer Code	14
Correlation with Experimental Data	19
References	24

EFFECTS OF TEMPERATURE ON FISSION-PRODUCT DEPOSITION

M. N. Ozisik

Abstract

An analytical model developed for steady state deposition of fission products from gas streams onto conduit surfaces is extended to include the effects of axial and radial temperature variations. A computer code which evaluates the equations is described and sample results are presented that compare the calculated values with experimental data.

Introduction

An investigation of the deposition of fission products from gas streams onto conduit surfaces in isothermal regions was reported previously.[1] In most applications, however, some regions are not always isothermal. In heat exchangers, for instance, both the gas and the wall surface temperatures vary with distance. In such regions the probability of a particle being deposited on the wall surface upon contact, the diffusion coefficients, and the mass transfer coefficients vary with distance. In addition, radial temperature gradients in the gas stream cause thermal diffusion, which enhances or retards the mass flux to the wall.

The effects of these factors on the steady-state deposition rate in nonisothermal regions were investigated analytically, and the resulting equations were programmed for a CDC 1604-A computer. The computer calculates deposition rates in isothermal regions followed by nonisothermal regions and makes a plot of the computed values and the experimental data for comparison. The equations presented are applicable for determining the deposition rates of fission products which enter the gas stream directly but not their daughter products.

Nomenclature

A	Cross-sectional area for flow, cm^2
a	Deposition surface per unit length of conduit, cm^2/cm
b	Linear rate of change of temperature in the nonisothermal region, °K/cm
C	Mass transfer coefficient obtained from heat-mass analogy, cm/sec
C_w	Mass transfer coefficient at the wall, cm/sec
$C^*_{1,2}$	Function defined by Eq. (33)
D	Diffusion coefficient, cm^2/sec
d_e	Equivalent passage diameter, cm
K	Ratio of thermal diffusion mass flux to ordinary diffusion mass flux as given by Eq. (2), dimensionless
L_1	Length of isothermal region, cm
L_T	Length of varying temperature region, cm
M	Concentration of particles on the wall surface, $particle/cm^2$
m	Molecular weight, g/g·mole
N	Precursor concentration in the gas stream at $x = 0$, $particle/cm^3$
n	Precursor concentration in the gas stream, $particle/cm^3$
P	Probability of a particle sticking on the wall upon collision, dimensionless
$\bar{p}$	Gas pressure, atm
Pr	Prandtl number, dimensionless
Q	Precursor deposition rate, $particle/cm^2 \cdot sec$
q	Adsorption energy, cal/g·mole
R	Gas constant, cal/g·mole·°K
Sc	Schmidt number, dimensionless
T	Temperature, °K
t	Time, sec
U	Gas velocity, cm/sec
x	Axial distance, cm
Z	Function defined in Eq. (33)
α	Function defined by Eq. (12)
α_t	Thermal diffusion factor, dimensionless

β	Viscosity variation coefficient, g/cm·sec·°K
ϵ/k	Lennard-Jones parameter for attraction energy of molecules, $°K^{-1}$
λ_0	Decay constant, sec^{-1}
μ	Viscosity, g/cm·sec
μ_d	Datum viscosity, g/cm·sec
ρ	Gas density, g/cm^3
σ	Lennard-Jones parameter for collision diameter, A
Ω	Collision integral, dimensionless
$\tau, \bar{\tau}$	As defined by Eq. (27), sec

Subscripts

I	Refers to the conditions at the isothermal region
g	Gas
o	Precursor
w	Wall

Basic Considerations

A local source was assumed to release fission products into a flowing gas stream in such dilute quantities that they exhibited no interference effects in diffusing or depositing on surfaces. The particles which entered the gas stream directly from the source are referred to hereafter, for convenience, as "precursors." It was assumed that the precursors were of uniform size and were so small that their motion in the gas stream was unaffected by gravitational and inertial forces and that they had no electric charges to affect deposition. Under such conditions, Brownian motion of the particles provides the principal mechanism for their transport across the laminar boundary layer to the wall surface. It has been shown[1] that the standard heat-mass analogy may be applied for estimating the rate of deposition of precursors from gas streams onto wall surfaces. For isothermal regions, the net mass flux (in particles/cm^2·sec) may be evaluated from[1]

$$Q_0 = P_0 C_0 N_0 \, e^{-\alpha_0 x} , \tag{1}$$

where

$$\alpha_0 \equiv \frac{1}{U_0}\left(\lambda_0 + \frac{4P_0C_0}{d_e}\right) .$$

In the following equations, the subscript, 0, which refers to the precursor, is omitted, for convenience.

In deriving Eq. (1), the mass transfer coefficient, C, and the probability factor for a particle to be deposited on the wall surface, P, were assumed to be constant, and no thermal diffusion effects were included. However, in regions such as heat exchangers, the temperature of the gas stream will vary both in the axial and radial directions. A radial force will be exerted on the particles because of the radial temperature gradient, and the resulting thermal diffusion will increase or decrease the deposition rate, depending on the direction of the temperature gradient. An approximate analysis[1] of the thermal diffusion component of the mass flux showed that it could be related to the ordinary diffusion component of the mass flux, as follows:

$$K \equiv \left(\frac{\text{Thermal diffusion mass flux}}{\text{Ordinary diffusion mass flux}}\right) = \alpha_t \left(\frac{Pr}{Sc}\right)^{1/3} \frac{T - T_w}{T + T_w} , \qquad (2)$$

where α_t is a thermal diffusion factor that is discussed later in this paper. In addition, there will be temperature effects on P and C. These effects are therefore included in the following derivations of the basic analytical relations for the deposition of precursors in nonisothermal regions. In the derivations, the subscript I denotes the isothermal region, and quantities without subscripts refer to the variable temperature region.

Derivation of Equations

A material balance equation for the concentration of precursors in the gas stream at a distance x from the origin (i.e., source) may be

stated as follows for the steady-state conditions:

$$\text{(Net rate of gain by convection)} - \text{(Rate of loss by decay)} - \text{(Rate of loss by deposition)} = 0 \ . \qquad (3)$$

Thus a material balance equation for a differential volume enclosed between x and x + Δx is

$$-\frac{d}{dx}(AUn)\,\Delta x - \lambda A\,\Delta x\,n - a\,\Delta x\,PCn(1 + K) = 0$$

or

$$\frac{d}{dx}(Un) + \left[\lambda + \frac{a}{A}PC(1 + K)\right] n = 0 \ . \qquad (4)$$

By definition,

$$d_e \equiv \frac{4A}{a} \ . \qquad (5)$$

Based on a constant flow area and a small pressure drop compared with the pressure level in the system, the gas velocity in the heat exchanger can be related to the gas velocity in the isothermal region as

$$U = U_I \frac{T}{T_I} \ . \qquad (6)$$

Substituting Eqs. (5) and (6) into Eq. (4) gives

$$\frac{d}{dx}(nT) + T_I \frac{1}{U_I}\left[\lambda + \frac{4PC}{d_e}(1 + K)\right] n = 0$$

or

$$n\frac{dT}{dx} + T\frac{dn}{dx} + T_I \frac{1}{U_I}\left[\lambda + \frac{4PC}{d_e}(1 + K)\right] n = 0 \ . \qquad (7)$$

Since the temperature distribution in a heat exchanger can often be approximated as

$$T = T_I + bx \ , \tag{8}$$

we set

$$\frac{dT}{dx} = b \ , \tag{9}$$

and Eq. (7) becomes

$$\frac{dn}{dx} + \frac{T_I}{TU_I}\left[\lambda + \frac{4PC}{d_e}(1 + K)\right] n + \frac{b}{T} n = 0$$

or

$$\frac{dn}{dx} + \left\{\frac{1}{U}\left[\lambda + \frac{4PC}{d_e}(1 + K)\right] + \frac{b}{T}\right\} n = 0 \ . \tag{10}$$

The solution of Eq. (10) with the boundary condition $n = N$ at $x = 0$ gives the concentration of the precursor in the gas stream at a distance x from the origin as

$$n = N \exp\left(-\int_0^x \alpha \, dx\right) \ , \tag{11}$$

where

$$\alpha \equiv \frac{1}{U}\left[\lambda + \frac{4PC}{d_e}(1 + K)\right] + \frac{b}{T} \tag{12}$$

The mass flux of the precursor to the wall surface, Q, can then be evaluated:

$$\begin{aligned} Q &= (\text{Ordinary diffusion mass flux}) + (\text{Thermal mass flux}) \\ &= (1 + K)\ (\text{Ordinary diffusion mass flux}). \end{aligned} \tag{13}$$

The mass flux resulting from ordinary diffusion can be obtained by making use of the heat-mass analogy, as follows:[1]

$$(\text{Ordinary diffusion mass flux}) = C(n - n_w) \equiv PCn \ , \tag{14}$$

where

$$P \equiv \frac{n - n_w}{n} \quad . \tag{14-a}$$

In Eq. (14), C is the mass transfer coefficient obtainable from standard heat transfer equations by analogy, n is the concentration of the precursor in the bulk free stream, and n_w is the concentration in the vicinity of the wall surface to within one mean free path. More will be said about the probability factor, P, later in this report.

Equations (11), (13), and (14) are combined to obtain the deposition rate (particles/cm^2·sec) in the nonisothermal region:

$$Q = PC(1 + K)\ N \exp\left(-\int_0^x \alpha\ dx\right) \quad . \tag{15}$$

The amount of precursor collected on the wall surface per unit area at time t after the start of deposition at the point considered is,[2] in particles/cm^2,

$$M = Q\ \frac{1 - e^{-\lambda t}}{\lambda} \quad . \tag{16}$$

For $\lambda t \ll 1$,

$$M \cong Qt \ , \tag{17}$$

and for $\lambda t \gg 1$,

$$M \cong \frac{Q}{\lambda} \quad . \tag{18}$$

Therefore, the concentration of precursors on the wall surface can be evaluated from Eq. (16) if the deposition rate, Q, is known. Equation (15) relates Q to position, x, but its evaluation depends on establishing the integrand α as a function of x. The various parameters in α that depend on temperature (and therefore on x) are U, C, P, and K. The manner in which temperature affects each of these is discussed below.

Coolant Velocity, U

The coolant velocity in the nonisothermal region is related to the coolant velocity in the isothermal region by Eq. (6), i.e.,

$$U = U_I \frac{T(x)}{T_I} \quad . \tag{6-a}$$

Mass Transfer Coefficient, C

The mass transfer coefficient can be obtained from heat transfer equations by an analogy for the type of flow and geometry under consideration.[1] For turbulent flow inside tubes, for instance,

$$\frac{Cd_e}{D} = 0.023 \left(\frac{U\rho d_e}{\mu}\right)^{0.8} \left(\frac{\mu}{\rho D}\right)^{0.3} \quad . \tag{19}$$

Since the physical properties of the gas vary with temperature, the following relations were used for evaluating density and viscosity as a function of temperature. For a perfect gas,

$$\rho = 1.22 \times 10^{-2} \frac{\bar{p} m_g}{T} \quad , \tag{20}$$

where

ρ = density, g/cm^3,
$\bar{p}$ = pressure, atm,
m_g = molecular weight of gas, and
T = temperature, °K.

Over a limited range, viscosity is assumed to vary linearly with temperature as

$$\mu = \mu_d + \beta T \quad , \tag{21}$$

where

μ = viscosity, g/cm·sec,
μ_d = a datum viscosity, g/cm·sec, and
β = a coefficient, g/cm·sec·°K.

A first approximation to the diffusion coefficient, D (cm^2/sec), is[3]

$$D = 0.185 \times 10^{-2} \frac{T^{3/2}}{\sigma^2 \bar{p} \Omega} \left(\frac{1}{m} + \frac{1}{m_g} \right)^{1/2} , \tag{22}$$

where

m, m_g = molecular weight of precursor and gas, respectively,
σ = the collision diameter, A,
Ω = dimensionless collision integral function.

The collision diameter, σ, is the distance of closest approach of two colliding molecules with zero initial kinetic energy and is slightly different from the molecular diameter used for the rigid sphere model in simple kinetic theory. The dimensionless function Ω relates to the deviation from the rigid sphere model for which it would be equal to unity at all temperatures. The values of Ω as a function of $T/(\epsilon/k)$ are available.[4] The Lennard-Jones parameters σ and (ϵ/k) for the combination of species i and j may be evaluated by combining the Lennard-Jones parameters for the individual species in the following manner:[3]

$$\left.\begin{aligned} \sigma &= \frac{1}{2} (\sigma_i + \sigma_j) \\ \frac{\epsilon}{k} &= \sqrt{\left(\frac{\epsilon}{k}\right)_i \left(\frac{\epsilon}{k}\right)_j} \end{aligned}\right\} . \tag{23}$$

Whenever possible the values of Lennard-Jones parameters for the individual species should be obtained from viscosity data; values are available for some species.[5,6] Data on Lennard-Jones parameters for the type of molecules of interest in fission-product deposition are rare, but they may be empirically estimated from the properties at the critical point, the boiling point, or the melting point.[7] For fission products entering the gas stream in atomic form, the value σ_j for the precursor may be taken as approximately equal to twice the atomic radius. Atomic radii are available in tabulated form for stable isotopes.[8]

Probability Factor, P

The probability of a particle depositing upon colliding with a wall surface was defined as

$$P = \frac{n - n_w}{n} \quad . \tag{24}$$

The reason for calling P the probability factor is given in the following explanation. The transport of particles from the bulk gas stream may be considered as being opposed by two resistances to mass transfer connected in series. The first is the resistance to mass transfer by diffusion, equal to $1/C$. After overcoming this resistance, particles come to within a distance of about one mean free path of the wall surface. From there, they collide with the wall surface by free flight. Since particles colliding with the wall surface do not all become permanently attached, a fictitious resistance to mass transfer, equal to $1/C_w$, can be assumed to exist there. Continuity of the mass flux across these resistances is expressed by

$$C(n - n_w) = C_w n_w$$

or, rearranging,

$$\frac{C_w}{C_w + C} = \frac{n - n_w}{n} \quad . \tag{25}$$

Comparing Eq. (25) with the definition of P in Eq. (24) gives

$$P = \frac{1}{1 + \frac{C}{C_w}} \quad . \tag{26}$$

It is apparent from this relation that P depends on the resistance to mass transfer at the wall surface, $1/C_w$, in such a manner that P tends to become unity as this resistance becomes zero and to become zero as the resistance at the wall becomes infinite. The resistance at the wall may be considered to be zero if all the particles colliding with the wall are

permanently attached to it or to be infinite if the particles do not stay on the wall surface at all. For this reason, P is referred to as the probability for the particles being attached or deposited on the wall surface. A perfect sink condition exists at the wall for P equal to unity and a perfect reflector exists for P equal to zero.

The temperature dependence of P was also investigated. According to Eq. (26), P depends on C and C_w. The manner in which the mass transfer coefficient C depends on temperature was discussed previously. The effects of temperature on C_w may be presumed with the following considerations. Collision of particles with the wall surface leads to a temporary binding of the particles on the wall surface. We may speak of physical adsorption if, in this act of binding, the individuality of the adsorbed molecule or the constituent parts of the surface is preserved, or of chemisorption if there is an interchange of molecules between the particles and the surface.[9] When a particle is not permanently attached, the average time it stays on the surface is[9]

$$\tau = \bar{\tau}\, e^{q/RT} \quad , \tag{27}$$

where τ is the time of oscillation of the molecules in the adsorbed state. The magnitude of $\bar{\tau}$ for various species appears to be of the order of 10^{-13} to 10^{-14} sec, and for a given species it can be considered as being constant. Therefore, the average time a given type of particle stays on a given type of surface is proportional to $e^{q/RT}$, where q is the adsorption energy in cal/g·mole and R is the gas constant in cal/g·mole·°K (i.e., 1.987).

The resistance offered to deposition because particles are not permanently attached to the wall surface may then be related to the temperature in the following form:

$$C_w = \text{constant} \cdot e^{q/RT} \quad . \tag{28}$$

The value of C_w in the varying temperature region may be related to the value C_{wI} in the isothermal region by

$$C_w = C_{wI} \exp\left[\frac{q}{R}\left(\frac{1}{T} - \frac{1}{T_I}\right)\right] \quad . \tag{29}$$

Substituting Eq. (29) into Eq. (26) gives the relation for P as a function of temperature in the region where the temperature varies with distance as

$$P = \frac{1}{1 + \dfrac{C_I}{C_{wI} \exp\left[\frac{q}{R}\left(\frac{1}{T} - \frac{1}{T_I}\right)\right]}} \quad . \tag{30}$$

C(T)

In the isothermal region $T = T_I$, and Eq. (30) becomes

$$P_I = \frac{1}{1 + \dfrac{C_I}{C_{wI}}} \quad , \tag{31}$$

where C_I is the mass transfer coefficient for diffusion in the isothermal region obtained by analogy from the heat transfer coefficient. Since no data are known to be available for the magnitude of C_w under the present conditions, C_{wI} was calculated, as follows, from experimental data for the isothermal region. Plotting the logarithm of the experimentally determined deposition in the isothermal region against distance should give a straight line, the slope of which is equal to the value of α_I. On the other hand, the value of α_I for the isothermal region, from Eq. (1), is

$$\alpha_I \equiv \frac{1}{U_I}\left(\lambda + \frac{4P_I C_I}{d_e}\right) \quad . \tag{32}$$

Since all the quantities, except P_I, in Eq. (32) are known, the value of P_I for the isothermal region can be calculated. Substituting this value into Eq. (31), the mass transfer coefficient for adsorption at the wall, C_{wI}, can be calculated.

Therefore, only q, the adsorption energy, is unknown in Eq. (30). If a suitable value is assigned to q, the variation of P as a function of temperature is completely defined. providing C(T) is known from 19, 20, 21, 22, & 23.

Diffusion Ratio, K

The ratio of the thermal diffusion to the ordinary diffusion is, from Eq. (2),

$$K = \alpha_t \left(\frac{Pr}{Sc}\right)^{1/3} \frac{T - T_w}{T + T_w} \quad . \tag{2}$$

The effects of temperature on the Prandtl and the Schmidt numbers in this equation can easily be determined, and the wall and gas temperatures are usually known. Values for the thermal diffusion factor, α_t, are rare, but approximate relations are available.[10,11] In most applications, fission products exist in the gas stream in small quantities, for which the first approximation to the thermal diffusion factor may be evaluated from[11]

$$\alpha_t = \left(6C_{12}^* - 5\right) \frac{5}{4\sqrt{2}} \frac{1}{Z} \quad , \tag{33}$$

where

$$C_{12}^* = \frac{\Omega_{12}^{(1,2)*}}{\Omega_{12}^{(1,1)*}} \quad ,$$

$$Z = \frac{\Omega_{22}^{(2,2)*} \sigma_{22}^2}{\Omega_{12}^{(1,1)*} \sigma_{12}^2} \quad .$$

The values of the dimensionless collision integrals, Ω^*, have been tabulated[12] as a function of $T/(k/\epsilon)$. For rigid spheres, the Ω^*'s are equal to unity, and Eq. (33) becomes

$$\alpha_t = \frac{5}{4\sqrt{2}} \left(\frac{\sigma_{12}}{\sigma_{22}}\right)^2 \quad , \tag{34}$$

where

σ_{12} = center-to-center distance between the colliding spheres,

σ_{22} = diameter of the lighter molecule (i.e., gas molecules for the present study).

Equation (33) is an approximation that is useful in making rough estimates for the thermal diffusion factor.

Computer Code

The deposition rate in the nonisothermal regions cannot be evaluated directly from Eq. (15) because the integrand, α, is a complicated function of temperature (and therefore distance), as explained above. A brief description of a computer program prepared[13] to evaluate this equation is given below.

For the calculation, a region of length L_1 is assumed where the temperature variation of the gas in the axial direction is negligible (i.e., b = 0), but a radial temperature difference is allowed to exist between the gas and the wall surface. Neglecting the variation of the integrand α with the axial distance, Eq. (15) becomes

$$Q_I(x) = P_I C_I (1 + K_I)\, N_I\, e^{-\alpha_I x} \qquad \text{for } 0 \leq x \leq L_I \ , \tag{35}$$

where

$$\alpha_I \equiv \frac{1}{U_I}\left[\lambda + \frac{4P_I C_I}{d_e}(1 + K_I)\right] .$$

This region will be referred to as the isothermal region, for convenience, and subscript I will refer to the conditions in this region.

The value of the mass flux is represented by $Q_I(0)$ for the isothermal region at the location x = 0 chosen as the origin. Equation (35) becomes

$$Q_I(x) = Q_I(0)\, e^{-\alpha_I x} \qquad \text{for } 0 \leq x \leq L_I \ . \tag{36}$$

In a varying temperature region of length L_T, where the gas temperature is assumed to vary both in the radial and axial directions, the deposition rate is given by

$$Q(x) = PC(1 + K)\ N \exp\left(-\int_0^x \alpha\ dx\right) \qquad \text{for } 0 \leq x \leq L_T\ , \quad (37)$$

where

$$\alpha \equiv \frac{1}{U}\left[\lambda + \frac{4PC}{d_e}(1 + K)\right] + \frac{b}{T}\ ,$$

and N is the gas stream concentration at the origin of the nonisothermal region. The origin, x = 0, is not the same point for the isothermal and nonisothermal regions, and therefore Q(0) is taken as the value of the deposition rate for the nonisothermal region at its origin. On the assumption that the nonisothermal region immediately follows the isothermal region, Eq. (37) gives

$$Q(0) = P_I C_I (1 + K_I)\ N \qquad (38)$$

and from Eqs. (37) and (38),

$$Q(x) = Q(0)\ \frac{PC(1 + K)}{P_I C_I (1 + K_I)} \exp\left(-\int_0^x \alpha\ dx\right) \qquad \text{for } 0 \leq x \leq L_T\ . \quad (39)$$

Equations (36) and (39) are programmed for evaluating the deposition rate as a function of the distance for an isothermal region followed by a nonisothermal region. These equations are coupled in such a manner that the end condition for Eq. (36) gives the condition at x = 0 for Eq. (39).

The deposition rate at x = 0 in the isothermal region, $Q_I(0)$, and the factor α_I are given as input data for solving these equations. From Eqs. (36) and (39), it can be seen that the input boundary condition may be given in terms of mass flux (particles/cm^2·sec) or particle concentration on the wall surface (particles/cm^2), and the results will be in like units.

A typical input data sheet for computer calculations is shown in Table 1. Table 2 shows a typical computer output sheet. The calculations are for the deposition of Zr^{95} from a turbulent helium stream on the inside of a 0.94-cm-ID tube. A 211.0-cm-long isothermal region (L_I) is followed by a 58.4-cm-long cooler region (L_T). The boundary condition at x = 0 for the isothermal region is given as $Dep_I = 1.5 \times 10^4$, and α_I is given as 0.00362. From the given α_I, the computer calculated the probability factor for the isothermal region as being $P_I = 0.37$. Deposition in the nonisothermal region is calculated by the computer for the adsorption energy q = 20,000 cal/g·mole. The computer output for the nonisothermal region is tabulated for six equally spaced locations. The values of the diffusion coefficient, D, the mass transfer coefficient, C, the mass transfer coefficient at the wall, C_w, the probability factor, P, the gas velocity, U, and the temperature, T, are all determined for each of these six locations.

A typical computer plot of deposition vs distance is shown in Fig. 1, which includes both calculated and input experimental data. In the

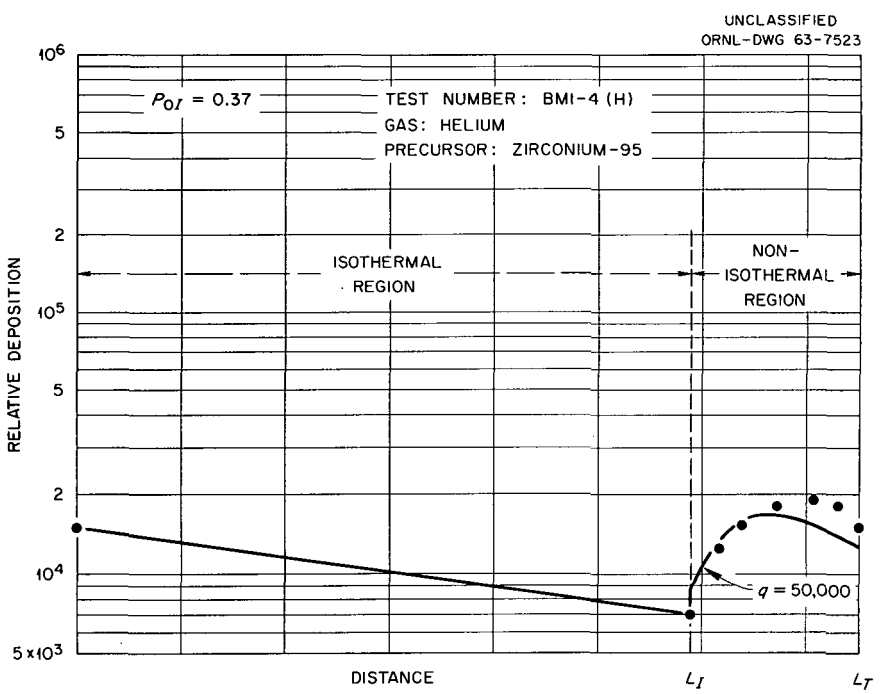

Fig. 1. Typical Computer Plot.

UNCLASSIFIED
ORNL-DWG 63-7521

TABLE 1. COMPUTER INPUT DATA SHEET

	1	26	46
1.	TEST NUMBER	GAS	PRECURSOR

	1	11	21	31	41	51	61	71
	Pr	m_g	m_0	σ	Ω	L_I	L_T	d_e
2.								

	1	11	21	31	41	51	61
	T_I	b	T_{wI}	T_{wt}	$\bar{p}$	U_I	α_t
3.							

	1	11
	α_{0I}	P_{0I}
4.		

	1	11	21	31
	μ_d	β	λ_0	Dep_{0I}
5.				

	1	4	7	10	13	16
	a	b	c	d	e	f
6.						

(SEE FOOTNOTE)

ISOTHERMAL EXPERIMENTAL DATA FOR LEAST SQUARES DETERMINATION OF α_{0I}

	#	X VALUES →					
	1 4	14	24	34	44	54	64
7a.							

	X VALUES →						
	1 11	21	31	41	51	61	71
7bi.							

	Dep VALUES →						
	1 11	21	31	41	51	61	71
7ci.							

	Dep VALUES →						
	1 11	21	31	41	51	61	71
7ci.							

	1
	p^*
8.	

	#	q VALUES →					
	1 4	14	24	34	44	54	64
9a.							

	q VALUES →						
	1 11	21	31	41	51	61	71
9bi.							

EXPERIMENTAL DATA TO BE PLOTTED

	#	X VALUES →					
	1 4	14	24	34	44	54	64
10a.							

	X VALUES →						
	1 11	21	31	41	51	61	71
10bi.							

	Dep VALUES →						
	1 11	21	31	41	51	61	71
10ci.							

	Dep VALUES →						
	1 11	21	31	41	51	61	71
10ci.							

FOOTNOTE:

a. INSERT 1 IF L_I FIRST
   INSERT 2 IF L_T FIRST
   INSERT 3 IF L_I ONLY
b. INSERT 1 IF LAMINAR
   INSERT 2 IF TURBULENT
c. INSERT THE NUMBER OF p^* VALUES
d. INSERT 1 IF q TO BE READ IN
   INSERT 2 IF LEAST-SQUARES FIT FOR q
e. FOR FUTURE USE
f. LEAVE BLANK IF NO GRAPH IS DESIRED
   INSERT 1 IF GRAPH DESIRED

TABLE 2. COMPUTER OUTPUT SHEET FOR Zr^{95}

TEST NUMBER BMI-4(H) GAS HELIUM PRECURSOR ZIRCONIUM 95

P*= .99

LI FIRST

DEPI (PART/SEC*CM**2)	MUI (G/CM*SEC)	TI (K)	RHOI (G/CM**3)	UI (CM/SEC)	LI (CM)	LT (CM)	LAMBDA (SEC**-1)	P (ATM)	B (K/CM)	DE (CM)
1.500E+004	4.417E-04	908.0	.001150	2280.0	211.0	58.4	.000	21.4	-3.00	.94

CALCULATED PHI= .37

ALPHAI= .00362 GIVEN VALUE

AT X=LI,DEP= 6.988E+03

OMEGA	SCHMIDT NO.	PRANDTL NO.	TW(ISOTHERMAL)	TW(TEMP. VARYING)	REYNOLDS NO.	AT
.950	2.269	.720	908	325	5581	.772

RATIO(ISOTHERMAL)= .000 RATIO(TEMP. VARYING)= .229

Q= 20000.000 GIVEN

	XT=0.0	XT=LT/5	XT=2LT/5	XT=3LT/5	XT=4LT/5	XT=LT
DEP,PART/SEC*CM**2	8.588E+003	1.062E+004	1.237E+004	1.343E+004	1.360E+004	1.299E+004
ALPHA,CM**-1	.00114	.00241	.00377	.00503	.00599	.00658
D, CM**2/SEC	.16927	.15957	.15006	.14075	.13163	.12273
CO, CM/SEC	5.26349	5.06439	4.86436	4.66337	4.46139	4.25840
CW, CM/SEC	3.07141	4.79269	7.76216	13.11185	23.23409	43.48588
CO/CW,	1.71370	1.05669	.62668	.35566	.19202	.09793
PO,	.36850	.48622	.61475	.73765	.83891	.91081
U, CM/SEC	2280.00000	2192.01410	2104.02819	2016.04229	1928.05639	1840.07048
T, K	908.00000	872.96000	837.92000	802.88000	767.84000	732.80000

isothermal region the calculated line obviously must coincide with the experimental data, because the input α_I and Dep_I were both taken from the experimental data.

The calculations for the nonisothermal region were for a value of adsorption energy q = 50,000 cal/g·mole. The solid curve shows the calculated values, and the small squares are the experimental points.

Discontinuity of the calculated curve at the beginning of the temperature-variable region is due to the stepwise introduction of the wall temperature change at this point. The radial temperature difference thus introduced causes, for the particular case investigated, a sudden increase in the deposition rate as a result of thermal diffusion.

Correlation with Experimental Data

The analytical model results were correlated with the test data obtained from out-of-pile experiments performed for ORNL at Battelle Memorial Institute. The experiments were performed in a 0.37-in.-ID type 304 stainless steel tube approximately 20 ft long. The precursors entered the helium stream from a fuel specimen consisting of enriched UC_2 particles in a graphite matrix. The fuel specimen had been irradiated prior to the test and stored to allow the short-lived fission products to decay. In the test loop, the fuel specimen was heated to 1800°F to accelerate the diffusion of fission products into the gas stream. The deposition test section consisted of a well-insulated isothermal region where the gas temperature was about 1200°F, followed by a cooler section where the gas temperature was reduced to 600°F.

There was scatter in the test data chiefly because of the presence of bends in the isothermal region. Smooth curves were drawn through the test points and used in the present correlation.

In performing the calculations for the nonisothermal region, the slope of the calculated curve was matched with the slope of the experimental curve in the isothermal region, and the boundary condition for the isothermal region was chosen as equal to the value of the measured deposition at x = 0. With the conditions thus specified, the calculated and the experimental curves were identical in the isothermal region. Calculations

were then performed for the nonisothermal region for the different values of α_t and q.

A parametric study was made to investigate the effects of the thermal diffusion factor, α_t, and the adsorption energy, q, on the calculated deposition curve in the nonisothermal region. Figure 2 shows the results of such a study for Zr^{95} with an assigned value of q = 50,000 cal/g·mole and α_t = 0, 1, and 2. Actual values of α_t are expected to be between 0 and 1. The calculated curve naturally has no discontinuity in transition from the isothermal to nonisothermal region for α_t = 0, but it shows a jump for the values of α_t = 1 and 2, where sudden increases in deposition of about 30 and 60%, respectively, occur for a gas-to-wall temperature difference of about 550°F assumed at the cooler inlet.

Figure 3 shows the effects of q on the shape of the calculated curve in the nonisothermal region for Ru^{103}. Calculations are for q = 0, 10,000, 20,000, 50,000, and 75,000 cal/g·mole with a value of α_t of about 0.8. It is apparent from Fig. 3 that the curvature of the calculated curve increases with increasing q; however, the rate of increase of the peak point of the curve is less at higher values of q.

Figures 4 through 7 are for the deposition of Ce^{141}, Ba^{140}, Te^{132}, and I^{135}. Calculations in the nonisothermal region were performed for q = 20,000, 50,000, and 75,000 cal/g·mole with an α_t of about 0.80. No attempt was made to determine the value of q that would best fit the calculated curve to the experimental values because the scatter in the actual test data from which the smoothed experimental points were obtained would not justify such a refinement. The general correlation of the experimental results with the calculated curves is reasonably good, however, if the q value is assumed to be between 20,000 and 50,000, for all the precursors considered, except I^{131}. It is apparent from Fig. 7 that the experimental points for the deposition of I^{131} in the cooler region are much higher than can be estimated with the present analysis, and the reason for this has not been explained. It is believed, however, that iodine might have formed a compound upon colliding with the cold wall that condensed or deposited at a much faster rate.

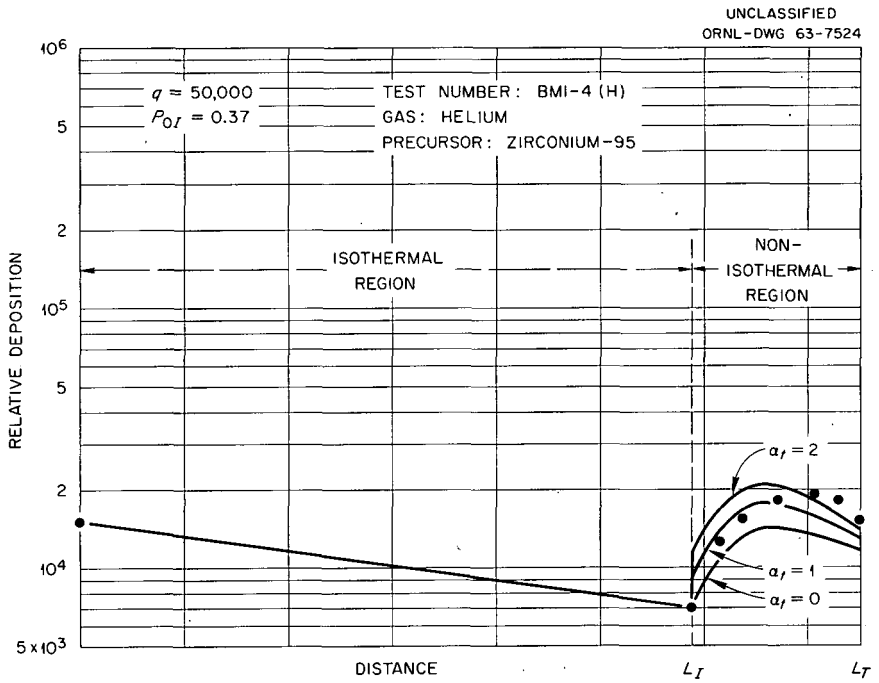

Fig. 2. Effects of Thermal Diffusion Factor, α_t, on Calculated Deposition in Nonisothermal Region.

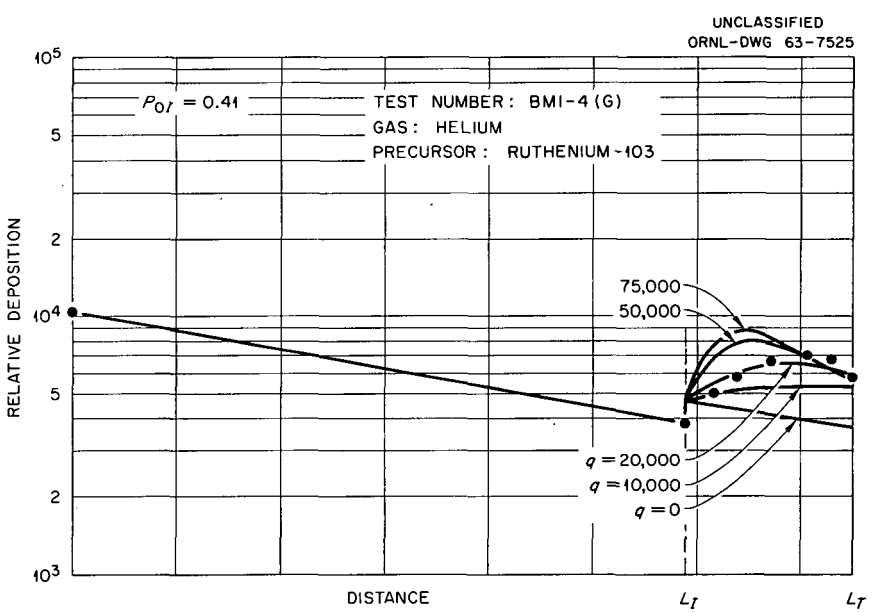

Fig. 3. Effects of Adsorption Energy, q, on Calculated Curve in Nonisothermal Region.

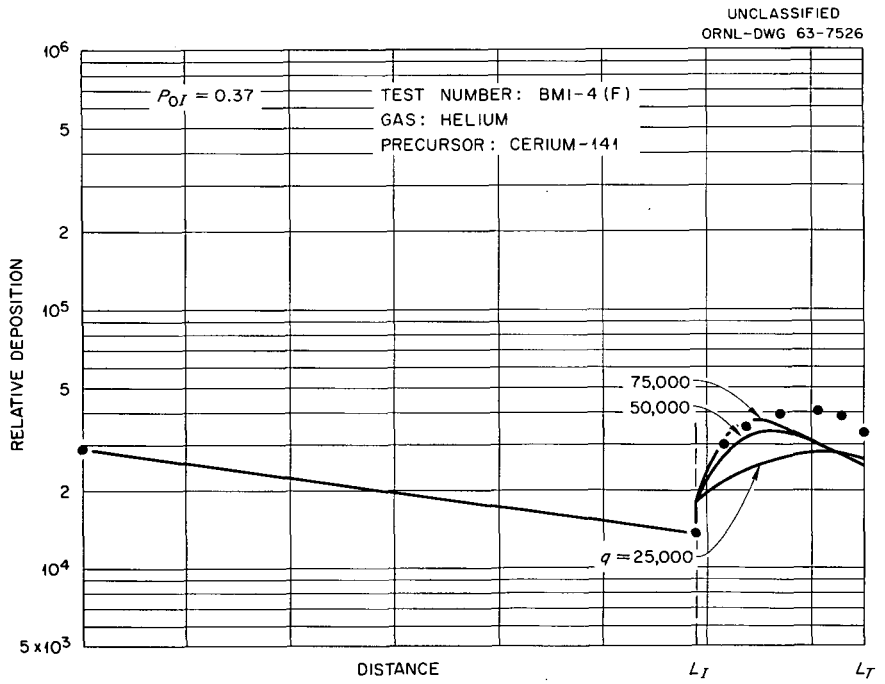

Fig. 4. Deposition of Cerium-141.

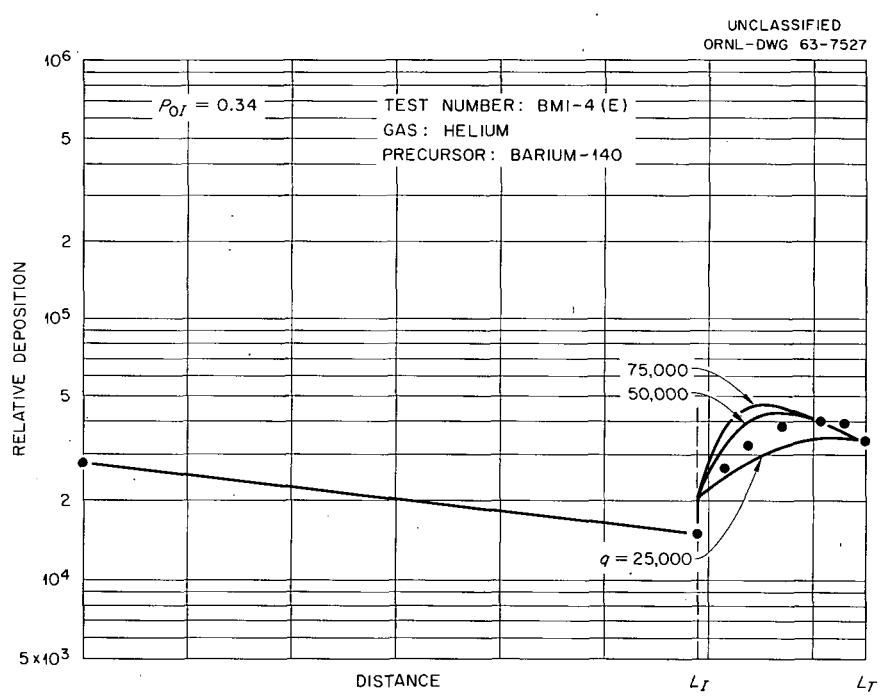

Fig. 5. Deposition of Barium-140.

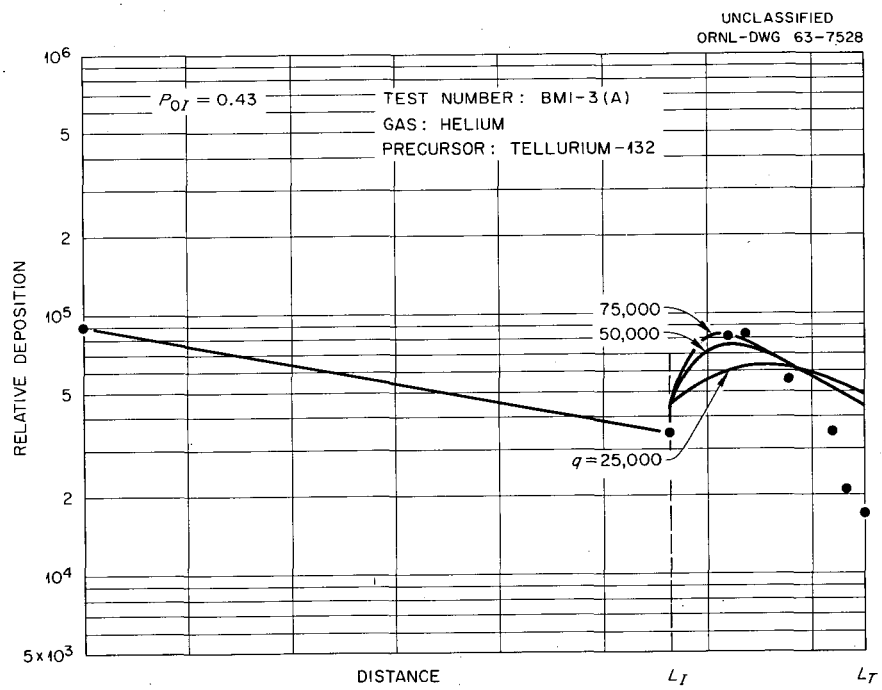

Fig. 6. Deposition of Tellurium-132.

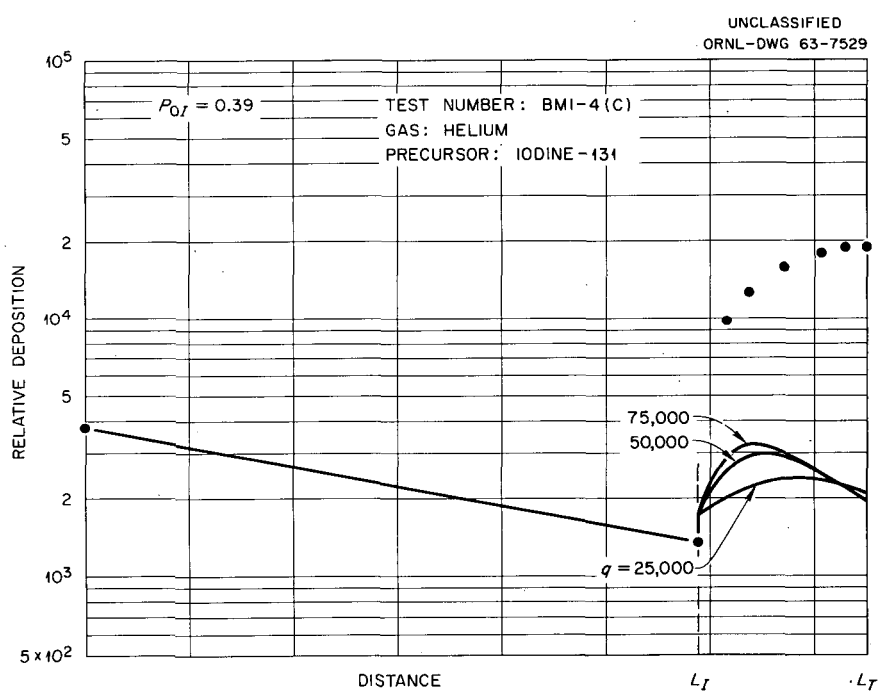

Fig. 7. Deposition of Iodine-131.

References

1. M. N. Ozisik, "An Analytical Model for Fission-Product Transport and Deposition from Gas Streams," USAEC Report ORNL-3379, Oak Ridge National Laboratory, July 26, 1963.

2. M. N. Ozisik, "A Transient Analysis of Fission Product Deposition," USAEC Report ORNL-TM-650, Oak Ridge National Laboratory, Oct. 1, 1963.

3. R. B. Bird, W. E. Stewart, and E. N. Lightfoot, p. 511 in Transport Phenomena, John Wiley & Sons, Inc., New York, 1960.

4. Ibid., p. 746.

5. Ibid., pp. 744–745.

6. J. O. Hirschfelder, C. F. Curtis, and R. B. Bird, pp. 1110–1112 in Molecular Theory of Gases and Liquids, John Wiley & Sons, Inc., New York, 1954.

7. R. B. Bird, W. E. Stewart, and E. N. Lightfoot, op. cit., p. 22.

8. T. Moeller, p. 135 in Inorganic Chemistry, John Wiley & Sons, Inc., New York, 1952.

9. J. H. de Boer, pp. 30–32 in The Dynamical Character of Adsorption, Oxford, Clarendon Press, 1953.

10. J. O. Hirschfelder, R. B. Bird, and E. L. Spotz, "The Transport Properties for Non-Polar Gases," The Journal of Chemical Physics, 16: 968–981 (1948).

11. S. C. Saxena and S. M. Dave, "Thermal Diffusion of Binary Gas Mixtures," Rev. Mod. Phys., 33(2): 148–152 (1961).

12. J. O. Hirschfelder, C. F. Curtis, and R. B. Bird, op. cit., pp. 1126–1127.

13. J. T. Beard, R. A. Hollister, and T. S. Kress, "A Code for Computing the Rate of Fission-Product Deposition from a Gas Stream," USAEC Report ORNL-TM-723, Oak Ridge National Laboratory (to be issued).

ORNL-3542

UC-80 - Reactor Technology
TID-4500 (26th ed.)

Internal Distribution

1. T. D. Anderson
2. S. E. Beall
3. C. D. Baumann
4. J. C. Bresee
5. W. E. Browning
6. R. M. Carroll
7. I. T. Dudley
8. W. F. Ferguson
9. B. R. Fish
10. W. R. Gall
11. D. A. Gardiner
12. P. A. Gnadt
13. F. F. Haywood
14. H. W. Hoffman
15. G. W. Keilholtz
16. J. J. Keyes, Jr.
17. R. N. Lyon
18. H. G. MacPherson
19. H. A. McLain
20. A. P. Malinauskas
21. W. D. Manly
22. J. F. Murdock
23. F. L. Parker
24. L. F. Parsly
25. M. W. Rosenthal
26. T. H. Row
27. G. Samuels
28. A. W. Savolainen
29. M. D. Silverman
30. O. Sisman
31. R. P. Shields
32. M. J. Skinner
33. R. S. Stone
34. D. B. Trauger
35. D. R. Vondy
36. C. D. Watson
37. R. P. Wichner

38–40. Central Research Library
41–43. Document Reference Section
44–68. Laboratory Records Department
69. Laboratory Records, RC

External Distribution

70–72. P. D. Bush, Kaiser Engineers
73. R. A. Charpie, UCC Research Administration, New York, N. Y.
74. W. R. Cooper, Tennessee Valley Authority
75–76. D. F. Cope, Reactor Division, AEC, ORO
77–78. R. W. Coyle, Vallecitos Atomic Laboratory
79. E. Creutz, General Atomic
80–82. R. B. Duffield, General Atomic
83. R. A. Ewing, Battelle Memorial Institute
84. H. L. Falkenberry, Tennessee Valley Authority
85. D. H. Fax, Westinghouse Atomic Power Division
86. M. Janes, National Carbon Research Laboratories, Cleveland, Ohio
87. T. Jarvis, Ford Instrument Co.
88. James R. Johnson, Minnesota Mining and Manufacturing Company, Saint Paul, Minn.
89. Richard Kirkpatrick, AEC, Washington
90. C. W. Kuhlman, United Nuclear Corp.

91–92. H. Lichtenburger, General Nuclear Engineering Corp.
93–95. S. Matovich, Allis-Chalmers Mfg. Co.
96. J. P. McGee, Bureau of Mines, Appalachian Experiment Station
97. R. W. McNamee, Manager, UCC Research Administration, New York, New York
98. M. N. Ozisik, North Carolina State University, Raleigh, N. C.
99. R. E. Pahler, Reactor Division, AEC, Washington
100. H. B. Rahner, Savannah River Operations Office
101. G. E. Raines, Battelle Memorial Institute
102. Corwin Rickard, General Atomic
103. M. T. Simnad, General Atomic
104. Nathanial Stetson, Savannah River Operations Office
105. Donald Stewart, AEC, Washington
106. S. A. Szawlewiez, AEC, Research and Development Branch, Division of Reactor Development
107. Philip L. Walker, Pennsylvania State University
108. R. E. Watt, Los Alamos Scientific Laboratory
109–110. W. L. Webb, East Central Nuclear Group, Inc.
111. C. E. Winters, UCC, Cleveland, Ohio
112. Lloyd R. Zumwalt, General Atomic
113. Division of Research and Development, AEC, ORO
114–725. Given distribution as shown in TID-4500 (26th ed.) under Reactor Technology category (75 copies – OTS)